JOURNAL OF VIROLOGY, Aug. 1997, p. 5922–5931 Vol. 71, No. 8
0022-538X/97/$04.00+0
Copyright © 1997, American Society for Microbiology

# Consequences of a Subtle Sialic Acid Modification on the Murine Polyomavirus Receptor

MARKUS HERRMANN,[1] CLAUS WILHELM VON DER LIETH,[2] PEER STEHLING,[3] WERNER REUTTER,[3] AND MICHAEL PAWLITA[1]*

*Angewandte Tumorvirologie[1] and Zentrale Spektroskopie,[2] Deutsches Krebsforschungszentrum, D-69120 Heidelberg, and Institut für Molekularbiologie und Biochemie, Freie Universität Berlin, D-14195 Berlin-Dahlem,[3] Germany*

Received 30 December 1996/Accepted 25 March 1997

**Polyomaviruses are small, nonenveloped DNA tumor viruses with restricted host ranges. Virus binding to cell surface receptors is one determinant of viral tropism. Although murine polyomavirus is among the best characterized viruses, little is known about the sialic acid-containing receptor and its interaction with viral particles. By using nonradioactive virus binding assays as recently described for the B-lymphotropic papovavirus, murine polyomavirus particles were found to bind in a saturable and noncooperative manner to 25,000 receptors per 3T6 mouse fibroblast. The virus-receptor interaction at 4°C was of high affinity ($K_d = 1.8 \times 10^{-11}$ M), very fast ($k_1 = 1.7 \times 10^7\ M^{-1}\ s^{-1}$), and stable (half-life = 38 min). Elongation of the *N*-acyl side chain of sialic acid by biosynthetic modulation with synthetic precursor analogs has been shown for other polyomaviruses to influence both sialic acid-dependent binding and infection (O. T. Keppler, P. Stehling, M. Herrmann, H. Kayser, D. Grunow, W. Reutter, and M. Pawlita, J. Biol. Chem. 270:1308–1314, 1995). In 3T6 cells in which about one-third of the sialic acids were modified, infection and binding of polyomavirus particles were significantly reduced. The number of receptors per cell was decreased to 18,000, with the remaining receptors displaying the same affinity as in untreated cells. Molecular modeling studies based on the three-dimensional structure of a mouse polyomavirus-sialyllactose complex recently solved by T. Stehle and coworkers (T. Stehle, Y. W. Yan, T. L. Benjamin, and S. C. Harrison, Nature 369:160–163, 1994) were performed. They suggest that the elongation of the *N*-acyl side chain by a single methylene group leads to steric hinderence, with the peptide backbone of a loop walling the tip of the shallow sialic acid binding groove. This collision appears to be incompatible with functional binding. The data are taken as a basis to discuss possible features of the organization and topology of the cellular receptor for mouse polyomavirus.**

Recognition of and stable binding to an appropriate receptor on the surface of the host cell by the virion is the first step of viral infection. Receptor recognition has to be selective and specific because virions bound to nonreceptor structures cannot initiate infection. Sialic acids (*N*-acetyl neuraminic acid [NeuNAc] or other N- and O-substituted neuraminic acids) are typical components of glycoconjugates on cell surfaces. Despite this ubiquity, such oligosaccharides appear to be an essential receptor component of many animal viruses from different virus families, such as influenza A and C viruses (orthomyxoviruses), Newcastle disease virus (paramyxovirus), cardioviruses (picornaviruses), and murine and primate polyomaviruses (papovaviruses) (4). For such viruses, enzymatic removal of sialic acids from cell surfaces leads to loss of virion binding, demonstrating the essential role of sialic acid for this initial step.

The complete natural receptor for any of these viruses has not been identified yet. On the other hand, the binding of sialic acid to virus surface proteins is well characterized, since the three-dimensional structures of two viral attachment proteins complexed with simple, monovalent sialylated saccharides, i.e., influenza A virus hemagglutinin (36, 37) and complete mouse polyomavirus (Py) (30, 31), have been solved. The binding affinity of the oligosaccharide ligands used in the crystal structures to their respective viral partner is rather weak, with dissociation constants ($K_d$s) of around $10^{-3}$ to $10^{-4}$ M (31, 36). This low affinity is in strong contrast to the high $K_d$ values of $10^{-8}$ to $10^{-12}$ M determined for the binding of complete virions from other virus species to cell surfaces (see reference 17 and references therein). It is still an open question how much of this high affinity is contributed by multivalent binding of the repetitive virion surface to repetitive oligosaccharide structures on the cell surface, on the one hand, or by binding to other, not-yet-identified structures on the viral receptor, on the other hand.

We have recently shown that synthetic D-mannosamine analogs with elongated *N*-acyl side chains can act as precursors for biosynthetically modified sialic acids. In tissue culture as well as in vivo, these compounds are taken up by cells, enter the sialic acid biosynthetic pathway, and result in glycoconjugates carrying sialic acids with elongated *N*-acyl side chains (19, 20, 39). When about 50% of the sialic acids were modified by the respective analogs, binding and/or infection of primate Pys that depend on cell surface sialic acids for entry were dramatically altered (20). For the human polyomavirus BK (BKV) the elongation of the *N*-acyl side chain by one methylene group (from *N*-acetyl to *N*-propanoyl) resulted in up to a sevenfold enhancement of infection, whereas further elongations to *N*-pentanoyl drastically reduced infection. For the African green monkey B-lymphotropic papovavirus (LPV), the minimally elongated *N*-propanoyl side chain already led to an approximately fivefold reduction of virus binding and over 10-fold reduction of infection. Cells with biosynthetically modified salic acids therefore represent a potent tool to analyze the

* Corresponding author. Mailing address: Angewandte Tumorvirologie, Abteilung 0615, Deutsches Krebsforschungszentrum, Im Neuenheimer Feld 242, D-69120 Heidelberg, Germany. Phone: (49) 6221-424645. Fax: (49) 6221-424932. E-mail: M.Pawlita@dkfz-heidelberg.de.

interaction of viruses with their sialylated host cell receptor in more detail.

The three-dimensional structure of crystals of Py complexed with sialyllactose has recently been solved (30, 31), providing a basis for an analysis of the sialic acid-virus interactions. The nonenveloped icosahedral Py consists of 72 pentamers of the major structural protein VP1 with one molecule of the minor structural protein VP2 or VP3 probably located within the pentamer center and protruding inwards the virion. There are five sialic acid binding sites per pentamer, with two neighboring VP1 molecules contributing to the shallow groove.

Here we describe in quantitative terms the binding of Py virions to host cells. To our knowledge this is the first case where affinity data for the binding of a virion to monovalent sialylated putative receptor fragments (30) and to host cell surfaces can be directly compared. Using biosynthetic modification of host cell sialic acid, we show that addition of a single methylene group to the *N*-acyl side chain, leading to a nonphysiological sialic acid, results in loss of binding and infection. Molecular modeling studies based on the crystal structure of the sialyllactose-Py complex strongly suggest that this inhibition is caused by steric hinderence due to a small structural change in the *N*-acyl side chains.

## MATERIALS AND METHODS

**Cells and viruses.** The murine embryonal fibroblast cell line 3T6 (33) and Py strain A2 (35) were kindly provided by G. Brandner, Freiburg, Germany. The cells were propagated as monolayers in plastic tissue culture bottles in Dulbecco's modified Eagle's medium (DMEM) with 5% heat-inactivated fetal calf serum, 2 mM glutamine, 100 U of penicillin per ml, and 100 μg of streptomycin per ml (cell culture medium) at 37°C in a humidified air with 5% $CO_2$. Cells were brought into suspension by incubation of the cell monolayer for 2 to 5 min in 0.2% (wt/vol) trypsin–0.2% (wt/vol) EDTA in phosphate-buffered saline (PBS). Viral infectivity was determined by end point titration on 3T6 cells.

**Virus infection and analysis of infected cells by indirect immunofluorescence.** 3T6 monolayer cells were washed once with cold PBS and were then incubated with Py stock virus at a multiplicity of infection (MOI) of 1 or 6 for 3 h at 4°C in DMEM without supplements. Unbound virus was removed by washing cells twice with precooled DMEM. After 24 h of cultivation in cell culture, Py-infected cells were detected by indirect immunofluorescence staining. Trypsin-suspended cells were allowed to settle on poly-L-lysine-coated slides (adhesion slides; Bio-Rad, Munich, Germany). Cells attached to the glass surfaces were fixed and permeabilized in cold methanol-acetone (1:1, vol/vol) at −20°C for 10 min. Viral antigens were first reacted for 30 min at 37°C with the Py viral protein (VP)-specific polyclonal rabbit antiserum (see below) and then stained with rhodamine-conjugated goat anti-rabbit immunoglobulins (Dianova, Hamburg, Germany). Nuclei were counterstained with DAPI (4′,6-diamino-2-phenylindole) (Boehringer Mannheim, Mannheim, Germany). All antibody dilutions and washings between antibody incubations were done in PBS.

**Treatment of cells with sialic acid precursor analogs.** The *N*-acyl-D-mannosamine derivatives *N*-acetyl-D-mannosamine (ManNAc), *N*-propanoyl-D-mannosamine (ManNProp), *N*-butanoyl-D-mannosamine (ManNBut), and *N*-pentanoyl-D-mannosamine (ManNPent) were synthesized and characterized as described previously (20), and 200 mM stock solutions in PBS were prepared shortly before use in cell culture. 3T6 mouse fibroblasts in exponential growth phase were freshly seeded and cultivated for 48 h in cell culture medium containing 20 mM *N*-acyl-D-mannosamine derivates. Cellular sialic acids were isolated, separated by high-pressure liquid chromatography, characterized by gas chromatography-mass spectroscopy, labeled with fluorescent markers, and finally quantitated as described previously (20).

**Purification of Py particles.** Py stock virus was added at an MOI of 5 to 3T6 mouse fibroblasts at approximately 10% confluency, and the cells were cultivated for 5 days. Suspended cells were centrifuged together with the tissue culture supernatant ($400 \times g_{av}$, 10 min, 4°C). The pelleted cells were washed once in PBS and were then suspended in 8 ml of extraction buffer (10 mM Tris-HCl [pH 7.5], 50 mM NaCl, 0.01 mM $CaCl_2$, 0.01% Triton X-100, 10 μg of aprotinin per ml) (9), and particles were extracted on ice by sonication three times for 20 s at level 5 with a Branson Sonifier 250. After incubation of the sonicated extract with sialidase from *Clostridium perfringens* (40 mU per $10^6$ cells; Boehringer, Mannheim, Germany) for 60 min at 37°C, cell debris was sedimentated for 10 min at $18,300 \times g_{av}$. Py particles in the supernatant were subsequently sedimentated (2.5 h, $180,000 \times g_{av}$, 20°C, Beckmann SW41Ti rotor) through 1.5 ml of 50% (wt/vol) sucrose in extraction buffer onto a 0.5-ml cushion of 80% (wt/vol) metrizamide (Gibco BRL, Eggenstein, Germany) (28) in extraction buffer. The metrizamide cushion and the sucrose-metrizamide interphase were collected (approximately 0.7 ml from each tube), pooled, adjusted to 43% (wt/vol) metrizamide, and subjected to equilibrium density gradient centrifugation (20 h, $150,000 \times g_{av}$, 10°C, Beckmann VTi65 rotor). Twenty-four fractions of approximately 250 μl each were collected from each gradient. The purification products were analyzed by silver-stained sodium dodecyl sulfate-polyacrylamide gel electrophoresis (SDS-PAGE), Py VP1-specific Western blotting, and enzyme-linked immunosorbent assay (ELISA) as well as by negative-staining electron microscopy as described previously for LPV (16, 17). Py VP1 was quantified by comparison of the silver-staining intensities of SDS-PAGE bands by using defined amounts of aldolase in the molecular weight marker (Mid-Range Protein Molecular Weight Markers; Boehringer Ingelheim Bioproducts, Heidelberg, Germany) as a reference. Total protein was quantified by the Bio-Rad protein assay.

**Py VP-specific antibodies.** A polyclonal rabbit antiserum against Py VPs was raised by subcutaneous injection of purified Py particles. An amount of particles corresponding to 100 μg of VP1 in 100 μl of PBS was suspended in the same volume of Freund's adjuvants (complete for the first injection and incomplete for the following two injections) at 4-week intervals.

Mouse monoclonal anti-Py VP1 antibodies were generously provided by R. A. Consigli (Manhattan, Kans.). To purify antibody D3 (23), 2 ml of 60 mM sodium acetate (pH 4.0) and 200 μl of caprylic acid were added per 1 ml of ascites fluid, and the suspension was stirred for 30 min at 20°C and afterwards centrifuged at $5,000 \times g_{av}$ for 10 min. After reextraction of the pellet in 40 mM sodium acetate (pH 4.0), the supernatants were pooled and dialyzed against PBS, and the protein fraction was precipitated in 50% ammonium sulfate, resuspended, and dialyzed against PBS.

**Quantitation of Py VP1 by ELISA.** The ELISA was constructed as described previously for the LPV VP1 ELISA (16, 17). Briefly, 150 ng of purified monoclonal anti-Py VP1 antibody D3 diluted in 100 μl of 50 mM sodium carbonate (pH 9.6) was applied as the catching antibody in wells of 96-well microtiter plates overnight at 4°C. PBS containing 0.05% (vol/vol) Tween 20 (PBS-Tween) was used throughout as a washing buffer between all incubation steps. Residual free protein binding sites on the plastic surfaces were blocked by incubation with 200 μl of 0.2% (wt/vol) casein in PBS for 3 h at 37°C. Incubation with 100 μl of viral antigen sample per well for 1 h at 37°C was followed by incubation with 100 μl of polyclonal rabbit Py VP-specific antiserum per well diluted 1:5,000 in 0.2% casein (Sigma, St. Louis, Mo.) in PBS-Tween and finally with 100 μl of peroxidase-labeled mouse anti-rabbit immunoglobulin G (heavy plus light chains) (Dianova, Hamburg, Germany) diluted 1:5,000 in the same buffer. A total of 100 μl of 100-μg/ml tetramethylbenzidine with 0.006% (vol/vol) $H_2O_2$ in 0.1 M sodium acetate (pH 6.0) was added as substrate. The reaction was stopped with 50 μl of 1 M $H_2SO_4$, and the absorbance at 450 nm was determined. The assay had a detection limit of 200 pg of Py VP1 per well.

**Py particle binding assays.** Py binding was determined by nonradioactive virus binding assays as described before for LPV (16, 17). Adherent cells in exponential growth phase were washed and were brought into a single-cell suspension by incubation in 5 mM EDTA in PBS for 10 min at 37°C. Cells were pelleted by centrifugation, resuspended in PBS containing 0.2% casein, and incubated with Py particles at 4°C for 60 min. After sedimentation of cell-virus complexes, either the amount of virus remaining in the supernatant (indirect binding assay, receptor in excess) or the amount of virus attached to the cells (direct binding assay, saturation binding) was quantified by Py VP1-specific ELISA. For indirect (receptor excess) binding assays, serially diluted cells were incubated with a constant amount of particles corresponding to 10 ng of Py VP1 in a final volume of 200 μl. For direct (saturation) binding assays, a constant number of cells ($1.2 \times 10^6$) was incubated with increasing amounts of particles in a final volume of 600 μl. The virus-cell suspension was layered carefully onto 500 μl of 8% (wt/vol) metrizamide over a 100-μl Ficoll-Paque (Pharmacia, Freiburg, Germany) cushion and centrifuged at $2,000 \times g_{av}$ for 10 min. Cells banded at the metrizamide–Ficoll-Paque interphase were collected with a needle and syringe and resuspended in an equal volume of lysis buffer (10 mM Tris-HCl [pH 7.5], 50 mM NaCl, 0.01 mM $CaCl_2$, 0.01% Triton X-100). Cells were further disrupted by sonication, and Py VP1 in the lysate was quantified by VP1-specific ELISA. Data were transformed by the method of Klotz (21) and plotted in a semilogarithmic graph, and binding parameters were calculated as described in detail previously (2, 17).

**Sialidase treatment.** To remove terminal sialic acids from cell surfaces, cultured cells were washed and suspended in EDTA (see above), and then $1.5 \times 10^6$ cells in 100 μl of PBS were incubated for 1 h at 37°C with 20 mU of *C. perfringens* sialidase (Boehringer), which preferentially cleaves (α2,3)-linked sialic acids. To remove sialidase prior to binding assays, cells were centrifuged and suspended in PBS-casein.

**Molecular modeling.** The X-ray structure of the VP1 monomer of murine Py complexed with (α2,3)-linked sialic acid at a resolution of 3.65 Å was kindly provided by T. Stehle and S. C. Harrison (30, 31), and modeling was performed by previously described methods. In brief, from a dimer of two VP1 units with sialyllactose as a ligand, a subset defining a sphere with a radius of 20 Å around the ligand and consisting of 189 residues and 2,938 atoms was cut out for computational studies. For all manipulations, the INSIGHTII software (Molecular Simulation/Biosym Technologies, San Diego, Calif.) was used. Missing H atoms were added, point charges were created for each atom by using the automatic charge assignment routine, and the potential types were assigned as needed for the consistent-valence force field (14, 15). The structures of the *N*-acyl analogs of NeuNAc were constructed interactively with the BIOPOLYMER

module of INSIGHTII by inserting methylene groups to the acetyl chain in such a way that no overlap with the protein surface occurred.

These model structures were then subjected to a molecular dynamic simulation with the program DISCOVER (Molecular Simulation/Biosym Technologies), consistent-valence force field, and the following protocol. All atoms belonging to residues more than 10 Å apart from the ligand were not allowed to move (first VP1 monomer, Ile79-Ala82, Ser89-Leu95, Ser160-His228, Gly245-Thr247, and Trp288-Tyr294; second VP1 monomer, Asn54-Gly69, Asp85-Thr86, Pro96-Ser99, Val130, Pro144-His163, Val178-Tyr185, Glu187-Thr195, Met201-His228, Gly246-Pro251, Cys282-Trp288, and Gly301-Pro303). The backbone atoms of the other residues were tethered with a force constant of 100 kcal/Å$^2$ (first VP1 monomer, Ala82-Ser89, and Asp180-Tyr185; second VP1 monomer, Gly69-Tyr73, Trp75-Pro96, His139-Lys143, and Arg289-Arg300). No constraints were applied to the side chains of the tethered residues or to any of the atoms of the ligands. A minimization of 1,000 steps by the conjugate gradient method was followed by an equilibration period of 20 ps and a production time of 100 ps. An integration step of 1 fs was used, and the coordinates were stored every 250 steps of integration. No explicit solvent molecules were included. A dielectric constant of 4 and a cutoff of 14 Å for the noncovalent interaction were applied.

The history of the molecular dynamic simulation was evaluated by automatically selecting the coordinates of the 10 structures with the lowest potential from the history files by using the program HIST_MIN (our software). These structures were subsequently subjected to an additional minimization, applying the conjugate gradient algorithm and the above-mentioned constraints. The minimization continued as long as the maximum derivative was greater than 0.001 kcal/Å$^2$, with a maximum of 10,000 steps. For the 10 optimized structures, the nonbonded interaction energies ($\Delta H_{binding}$) were calculated by using the ENCLOSE option of DISCOVER. To evaluate the relative strain of the ligand molecules bound to the protein, the total energy ($\Delta H_{conform}$) was calculated for each of the 10 selected isolated ligand structures. Recently, a similar modeling protocol was successfully applied to mimic the calculated relative binding energies of a series of NeuNAc analogs binding to the sialidase from influenza virus (32).

## RESULTS

**Reduction of Py infection by elongation of the *N*-acyl chain of sialic acid.** When mammalian cells are cultivated in the presence of N-substituted D-mannosamine derivatives, they can take up these compounds and metabolize them in the sialic acid biosynthetic pathway (13, 19, 20). As a consequence, structurally altered sialic acids with substituted *N*-acyl side chains are incorporated into various glycoconjugates (18, 19). As we have shown recently (20), infection and binding of the human BKV and of the African green monkey LPV, both of which use sialidase-sensitive cell receptors (16, 29), are altered in cells in which up to 50% of the sialic acids are biosynthetically modified and carry elongated *N*-acyl side chains. Addition of a single methylene group to yield *N*-propanoyl-substituted neuraminic acid instead of the physiological *N*-acetyl-substituted neuraminic acid in Vero cells resulted in strong enhancement of BKV infection and probably also in BKV binding, whereas further elongation of the *N*-acyl chain nearly completely inhibited virus uptake. Infection of the same cells by simian virus 40 (SV40), whose uptake is sialic acid independent (8), remained unaltered. For LPV, the *N*-propanoyl derivative already drastically reduced infection and lowered the virus binding capacity of the treated cells fourfold (20).

Mouse Py also uses a sialidase-sensitive receptor (5, 6). In addition, the crystal structure of Py with a sialic acid-($\alpha$2,3)-lactose bound to it has been solved (30), thus providing an excellent basis for the analysis of sialic acid-dependent virus-receptor interactions in detail.

We first tested whether infection by Py, like that by BKV and LPV, also is sensitive to elongation of the *N*-acyl chain on cellular sialic acids. The murine fibroblast line 3T6 was used as the host cell. Prior to Py infection, the cells were pretreated for 48 h with the synthetic sialic acid precursor analogs. To generate sialic acids with elongated *N*-acyl side chains, ManNProp, ManNBut, and ManNPent were used. The physiological precursor analog ManNAc served as control. For ManNProp and ManNBut pretreatment, the identity and the amount of incorporated modified sialic acids were determined as described previously (20). In the case of ManNProp pretreatment, 35% of the cellular sialic acids extracted contained the modified *N*-acyl group, and in ManNBut-pretreated cells, 37.5% did (data not shown). At 48 h postinfection, cells were harvested and the fraction of Py-infected cells was quantified by indirect immunofluorescence staining of viral proteins. When infected at an MOI of 1, cultures pretreated with the physiological precursor ManNAc showed about 12% VP-positive cells and were nearly indistinguishable from untreated cultures, with 13.6% VP-positive cells. In contrast, in all three cultures pretreated with nonphysiological sialic acid precursor analogs, only about 3 to 5% of the cells were VP positive, which indicates a reduction of infection by 64 to 78% (Fig. 1). At an MOI of 6, untreated and ManNAc-pretreated cells showed about 27 and 30% VP-positive cells, respectively, and ManNProp- and ManNBut-pretreated cells showed about 4% VP-positive cells, indicating a reduction of infection of approximately 85%.

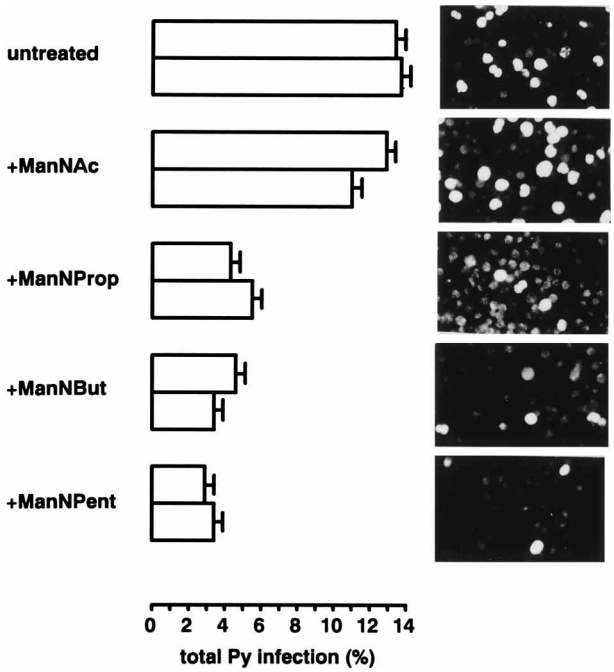


FIG. 1. Reduction of murine Py infection in 3T6 cells by sialic acids with elongated *N*-acyl chains. Infection in 3T6 cells (MOI of 1) pretreated with synthetic *N*-acyl elongated D-mannosamines (ManNProp, ManNBut, and ManNPent) is compared to that in untreated cells and cells pretreated with the physiological precursor ManNAc. Panels on the right show representative Py-specific immunofluorescence of infected cells for each treatment. Bars on the left give the percentage of immunofluorescence-positive cells and are the arithmetic means ± standard deviations from three independent determinations in two separate experiments.

**Fast and high-affinity binding of Py to 25,000 sialylated receptors on unmodified 3T6 cells.** In order to test whether the reduction of Py infection by the modified sialic acids is mediated by a reduction in virus-receptor interaction, binding assays using purified virus particles and nonradioactive virus quantitation by VP-specific ELISA were developed. Similar quantitative binding assays have been described previously for LPV (16, 17). Since to our knowledge these binding parameters have not been determined yet for any Py-host cell pair, the results are first described in detail for normal 3T6 cells with unmodified sialic acids. Five binding characteristics, i.e., receptor number per cell, dissociation constant ($K_d$), association rate

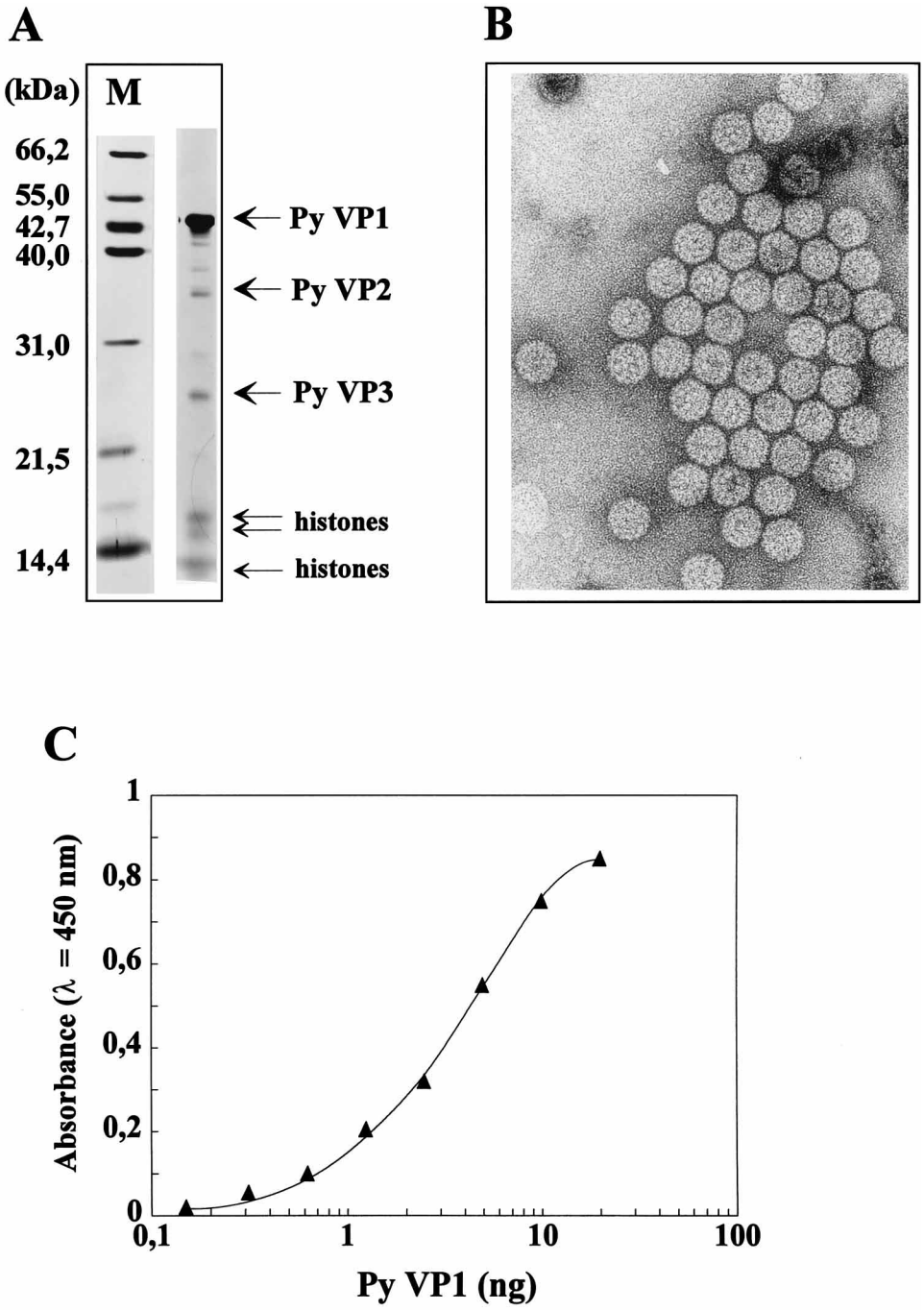


FIG. 2. Purity and integrity of Py particles used for binding assays and detection range of the VP1-specific ELISA. (A) After step gradient and equilibrium density gradient centrifugations, pooled particle-containing fractions were analyzed by SDS-PAGE and silver staining of proteins. Lane M contained the size marker. Arrows on the right indicate the positions of the Py structural proteins VP1, VP2, and VP3 as well as cellular histones associated with the viral genome. (B) Electron micrograph of negatively stained purified Py particles. Particle diameter is approximately 45 nm. (C) Typical titration curve of Py particles in the VP1 catching ELISA.

constant ($k_1$), dissociation rate constant ($k_2$), and half-life ($t_{1/2}$) of the virus-receptor complex were determined.

Py virions were extracted from Py-infected 3T6 mouse fibroblasts by sonication in low-salt and low-detergent buffer, and virion-attached receptors were removed by incubation with sialidase from *C. perfringens*. Py particles were purified by centrifugation through a 50% sucrose cushion followed by metrizamide equilibrium density gradient ultracentrifugation as described for LPV particles (16, 27). The high purity of the resulting particle preparation was demonstrated by silver staining of proteins separated by SDS-PAGE. Proteins with the expected apparent molecular masses (11) of the major structural proteins VP1 (47 kDa), VP2 (35 kDa), and VP3 (23 kDa) as well of histones (17 to 14 kDa) made up more than 95% of the stained bands (Fig. 2A). The 47-kDa protein was additionally identified as VP1 by its reactivity in Western blots with a polyclonal anti-Py VP1-specific antiserum (not shown). The integrity of the virions was apparent by negative-staining elec-

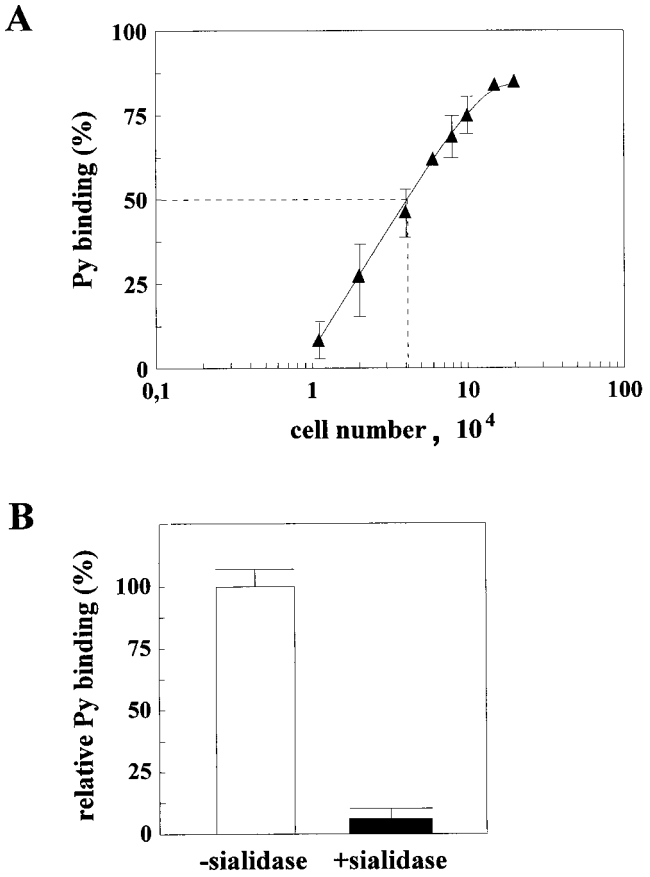


FIG. 3. Py binding to 3T6 cells under conditions of receptor excess. (A) A constant amount of Py particles (corresponding to 10 ng of Py VP1) was incubated with increasing numbers of untreated 3T6 cells, and the fraction of virus bound was determined by an indirect binding assay. Dashed lines indicate the binding capacity, i.e., the cell number that binds 50% of the virus administered. Each data point is the arithmetic mean ± standard deviation from at least three independent determinations. (B) Relative binding of Py particles to $10^5$ 3T6 cells pretreated with or not pretreated with *C. perfringens* sialidase.

tron microscopy (Fig. 2B). We estimated that from 1 liter of cell culture, viral particles corresponding to about 6 mg of Py VP1 could be purified.

For quantitation of Py particles, a Py VP1-specific catching ELISA, analogous to the recently described LPV VP1-specific ELISA (16) but less sensitive, with a detection range of approximately 0.2 to 20 ng of Py VP1 (Fig. 2C), was established.

Py binding to 3T6 mouse fibroblasts was first determined qualitatively by indirect binding studies. Cells were brought into suspension by incubation in EDTA, washed, and incubated for 1 h at 4°C under gentle agitation with a constant amount of Py particles. After sedimentation of cell-bound virus by low-speed centrifugation, Py particles remaining in the supernatant were quantified by the Py VP1-specific ELISA. With a high excess of receptors, more than 90% of the Py VP1 antigen bound. With 10 ng of Py particles administered, 50% binding was reached by $4 \times 10^4$ cells (Fig. 3A). Sialidase sensitivity of Py binding was confirmed with 3T6 cells pretreated with sialidase from *C. perfringens*. In such cells the binding activity (Fig. 3B) and the infectability (not shown) were reduced to about 10% of those of untreated cells.

The number of Py receptors per 3T6 mouse fibroblast and their affinity were determined by direct binding assays under conditions of virus excess. Py particles were incubated with suspended cells. Cell-bound virus was separated from free virus by low-speed sedimentation of the cells on a Ficoll-Paque cushion and quantified in the lysate by VP1-specific ELISA. Saturation analysis showed a hyperbolic binding curve, which indicates a homogeneous set of saturable, noncooperating receptors (Fig. 4A). Scatchard transformation of these primary data (not shown) yielded a straight line. However, due to the experimental variation of the binding assays, a rather low regression coefficient ($r$) of −0.90 resulted, which indicated a high and not acceptable degree of imprecision. Therefore, as applied and discussed previously (17), the receptor number per cell was determined by the more robust method of Klotz (21) (Fig. 4B). The sigmoidal graph of the semilogarithmic plot at the turning point indicated half-maximal saturation at 12,500 Py particles bound per cell and approached asymptotically a value of maximal binding of 25,000 Py particles bound per cell, which equals the number of functional receptor sites per cell. The calculated dissociation constant, $K_d$, was $1.8 \times 10^{-11}$ M, a value indicating a high affinity (see reference 17 for comparisons). The calculation was based on the equation $K_d = R_{cell} \cdot C \cdot V_f/V_b$ and uses the receptor number per cell ($R_{cell}$) determined in the Klotz plot and the concentrations of free ($V_f$) and bound ($V_b$) virus and of cells ($C$) at 50% binding in the indirect binding assay (Fig. 3A) as described recently in detail for the determination of LPV binding parameters (17).

The kinetics of Py binding was examined under conditions of receptor excess. The extrapolation of the slope of the initial binding reaction resulted in a time ($t$) of approximately 12 min for total virus binding (Fig. 4C). The association rate constant $k_1 = 1.7 \times 10^7\ M^{-1}\ s^{-1}$ was calculated from the equation $k_1 = (R \cdot t)^{-1}$, where $R$ represented the free receptor concentration of $8.1 \times 10^{-11}$ M at the beginning of the analysis. The dissociation rate constant, determined from the equation $k_2 = K_d \cdot k_1$, was $3.1 \times 10^{-4}\ s^{-1}$, yielding a $t_{1/2}$ of 38 min for the Py-receptor complex. Thus, the interaction of Py with its cellular receptor on mouse fibroblasts is of high affinity, fast, and stable.

**Reduction of the number of functional Py receptors by elongation of the neuramic acid *N*-acyl side chain.** We first analyzed whether the infection inhibition observed in cells with modified sialic acids correlated with changes in virus binding to such cells. In indirect binding assays the number of cells needed to bind 50% of the virus administered was determined. Untreated cells and cells pretreated with the physiological precursor ManNAc showed similar binding capacities, whereas cells with modified sialic acids had only 15 to 40% of the binding activity of untreated cells (Fig. 5). Thus, for cells with modified sialic acids, both virus infection and binding were reduced to very similar extents.

Since all three precursor analogs with elongated *N*-acyl side chains showed similar inhibition and binding reductions, more detailed binding studies in parallel with untreated cells were performed only with the analog that had the smallest structural difference from the physiological sialic acid, i.e., ManNProp. We wanted to determine whether the reduction of virus binding seen before was due to a decrease in the number of functional Py receptors, a decrease in affinity of the Py-receptor interaction, or both.

The Py receptor number on ManNProp-pretreated cells was quantified in direct binding assays under conditions of virus excess. The saturation data (Fig. 6A) are shown replotted according to the method of Klotz (Fig. 6B), because Scatchard analysis could not be fitted satisfactorily on a straight line. The value of $n$ = 18,000 particles bound per cell equals the number of Py receptor sites per ManNProp-pretreated 3T6 cell and is 28% lower than the number of receptors on untreated cells.

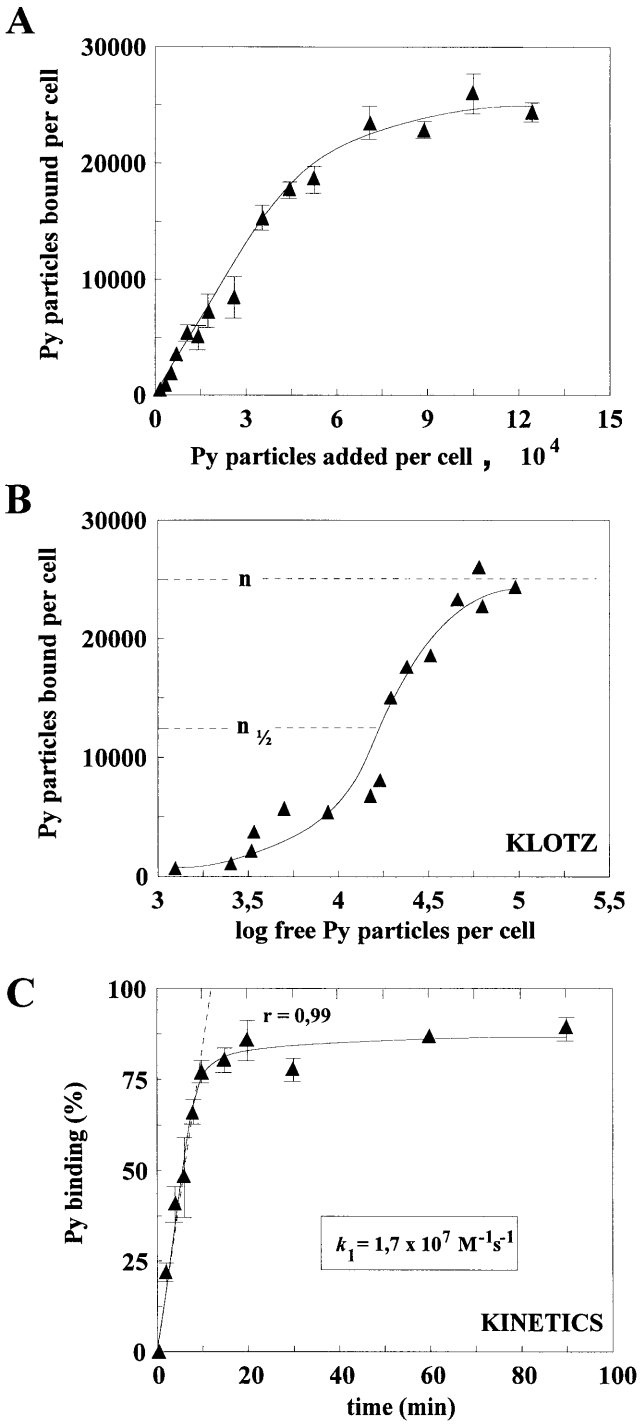


FIG. 4. Quantitative parameters of Py binding. (A) Saturation binding of Py particles to 3T6 cells was determined by a direct binding assay under conditions of virus excess. The number of particles bound per cell was plotted against the number of particles added. (B) The primary data of panel A were transformed by the method of Klotz. $n_{1/2}$ indicates the half-maximum number of receptors per cell at the turning point of the sigmoidal curve; n is the total number of receptors per cell. (C) The association kinetics of Py receptor attachment at 4°C were determined by an indirect binding assay under conditions of receptor excess ($R = 8.1 \times 10^{-11}$ M). The dashed line indicates the extrapolated initial binding curve intersecting 100% Py binding at $t = 12$ min. The association rate constant $k_1 = 1.7 \times 10^7$ $M^{-1}$ $s^{-1}$ was calculated from the equation $k_1 = (R \cdot t)^{-1}$. The initial six data points can be fitted on a straight line with a regression coefficient ($r$) of 0.99. Each data point is the arithmetic mean ± standard deviation from three independent determinations.

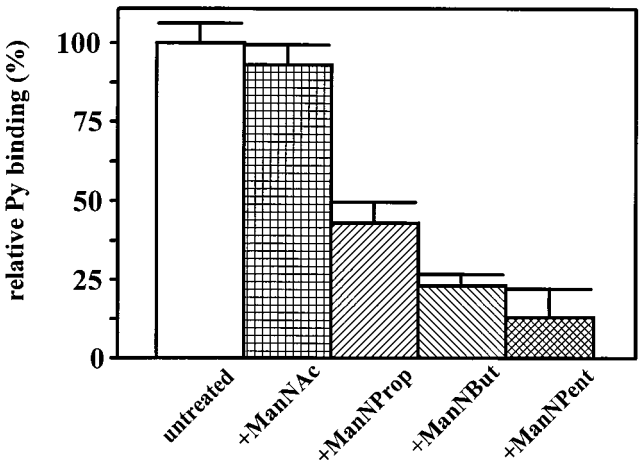


FIG. 5. Reduction of Py binding by sialic acids with elongated *N*-acyl side chains. Py binding to 3T6 cells pretreated with synthetic *N*-acyl-elongated D-mannosamines (ManNProp, ManNBut, and ManNPent) is compared to that of untreated cells and cells pretreated with the physiological precursor ManNAc. Values given are the amount of Py bound by treated cells relative to that bound by the same number of untreated cells. Each value is the arithmetic mean ± standard deviation from three independent determinations.

To determine the dissociation constant ($K_d$) for the Py-receptor interaction on ManNProp-pretreated cells, the cellular binding capacity was quantified by indirect binding assays (Fig. 6C), and, as described above for untreated cells, a $K_d$ value of $1.8 \times 10^{-11}$ M was calculated. This is equal to the dissociation constant determined for the Py-receptor interaction on untreated cells.

Thus, the incorporation of approximately 35% sialic acids with an elongated *N*-acyl side chain resulted in a reduction of the number of viral receptors of approximately 28%.

**Molecular modeling of the interaction of mouse Py VP1 with *N*-acyl-modified sialic acids.** The results of the binding experiments had suggested that cellular Py receptors carrying analogs of NeuNAc with elongated *N*-acyl side chains could no longer bind the virus. Since the crystal structure of Py in complex with sialyllactose as a receptor fragment has been solved (30, 31), we applied molecular modeling techniques to analyze the effects of *N*-acyl side chain elongation on this complex. For each of the three analogs, 10 structures optimized for minimal potential energy were calculated by molecular dynamic simulation. Upon overlay and visual inspection, all calculated structures appeared similar and showed the same basic differences from the crystal structure with NeuNAc lactose.

The spatial topology of a representative structure calculated for *N*-propanoyl neuraminic acid lactose (Fig. 7, bottom) is shown together with the established crystal structure of the physiological complex of NeuNAc lactose with Py (Fig. 7, top). In the latter complex the *N*-acetyl group fits tightly into the bottom of the binding groove and is surrounded on four sides by rather high walls. In contrast, the fitted *N*-propanoyl derivative shows drastic differences. The *N*-propanoyl group is no longer in the bottom of the binding pocket but is bent upwards. The neuraminic acid is tilted around the (α2,3)-glycosidic linkage (magenta arrow) and pushed towards the right. Thus, the highly charged carboxylate group (yellow arrow), which provides the bulk of the binding energy by its interaction with the guanidinium group of arginine 77 (31), is moved away from its binding partner. The elongation of the *N*-acetyl side chain apparently resulted in considerable conformational stress on the ligand and in loosening of the interaction that NeuNAc has with the virus surface.

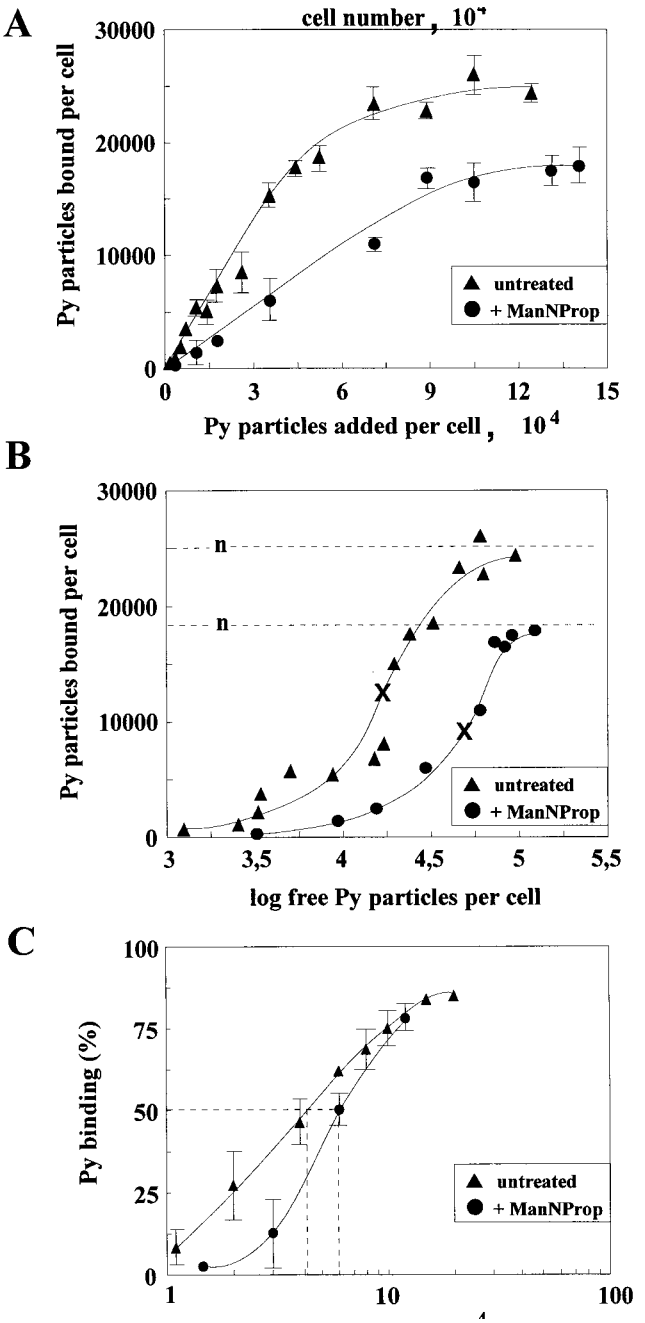


FIG. 6. Reduction of the number of functional Py receptors in cells carrying *N*-propanoyl neuraminic acids. (A and B) Saturation binding curve for untreated (data from Fig. 4) and ManNProp-pretreated cells (A) and transformation by the method of Klotz (B). For further details, see the legend to Fig. 4. (C) In indirect binding assays under conditions of receptor excess, increasing numbers of 3T6 cells were incubated with constant amounts of Py particles (10 ng corresponding to Py VP1). Dashed lines indicate the points were 50% of the virus administered was bound and are an indication of the cells' binding.

This visual interpretation is supported by empirical molecular mechanics energy calculations which were performed for each of the generated structures to quantify the effects of the structural changes. The rationale and details of the modeling protocols and energy calculations shall be published elsewhere. In brief, three types of energies were calculated: $\Delta H_{\text{binding}}$ encompasses van der Waals, electrostatic, polar, and hydrogen bond interactions between the virus and the oligosaccharide; $\Delta H_{\text{conform}}$ describes the conformational strain of the ligands in the bound state; and $\Delta S_{\text{flex}}$ covers the unfavorable entropy changes associated with the freezing of torsional angles in the bound state. For all three modified sialic acids and for all three types of energies analyzed, the calculated differences relative to the physiological NeuNAc are grossly unfavorable for binding. Any elongation of the *N*-acetyl group is possible only when the ligand exhibits an unusual conformation of this functional group as well as of the complete ligand. In all complexes with elongated ligands, the free energy ($\Delta G$) appears to be reduced

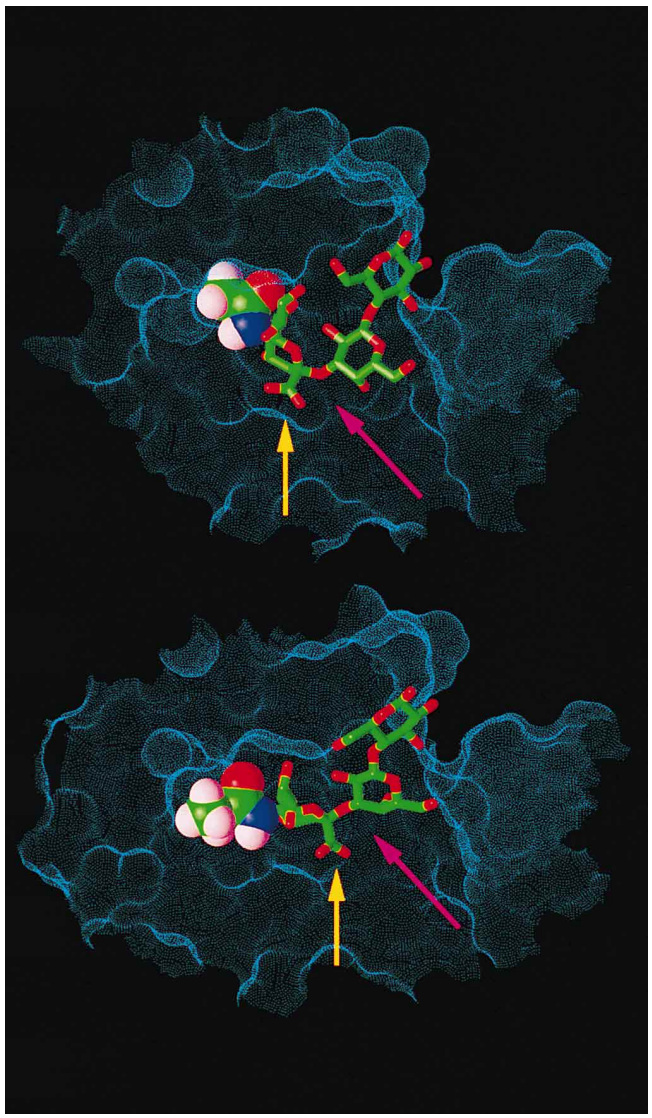

FIG. 7. Receptor binding site of Py complexed with *N*-acetyl (top) and *N*-propanoyl (bottom) neuraminic acid lactose. The structure of the *N*-acetyl complex is based on the X-ray structure of Stehle et al. (30, 31); the *N*-propanoyl complex structure (one representative of 10 similar ones calculated) was derived from the X-ray structure by molecular dynamic simulation. The protein surface is shown by light blue dots, and the oligosaccharide is shown as a stick model with the H atoms omitted. The *N*-acetyl and *N*-propanoyl groups of the neuraminic acid are shown as space-filling models including the H atoms. C atoms are shown in green, O atoms are in red, H atoms are in white, and the N atom of the neuraminic acid is in dark blue. The carboxylate residue is indicated by a yellow arrow, and the (α2,3)-glyosidic linkage connecting the neuraminic acid with lactose is indicated by a magenta arrow.

by 20 kcal/mol as compared to that of the physiological NeuNAc. Since a difference in free energy of 1.4 kcal/mol corresponds to 1 order of magnitude for the binding-dissociation constant, it can be estimated for all three sialic acid variants that their affinity for VP1 is several orders of magnitude lower than that of the physiological NeuNAc.

## DISCUSSION

Py virions bind to the surface of murine 3T6 fibroblasts with high affinity. We have determined here a dissociation constant of $1.8 \times 10^{-11}$ M for the interaction of a Py particle with a cell surface site that functions as a virus receptor. This $K_d$ value indicates that the affinity of Py-receptor binding is approximately fivefold lower than that of SV40-receptor binding ($K_d = 3.8 \times 10^{-12}$ M [7]) and sixfold lower than that of LPV-receptor binding ($K_d = 2.9 \times 10^{-12}$ M [17]). Py binds to 25,000 receptors per 3T6 fibroblast, as compared to 1,800 LPV receptors on a human B-lymphoma line cell (17) and to 90,000 SV40 receptors on Vero monkey kidney epithelium cells (7). Unpublished data cited in reference 3 suggested that there are 10,000 specific Py receptor sites on quiescent primary mouse kidney cells.

The Py-receptor interaction at 4°C not only was of high affinity but also was very fast, with an association rate constant of $1.7 \times 10^7$ $M^{-1}$ $s^{-1}$, and stable, with a virus-receptor complex $t_{1/2}$ of 38 min. Similar values have been determined previously for LPV-receptor complexes at 37°C ($k_1 = 6.7 \times 10^7$ $M^{-1}$ $s^{-1}$ and $t_{1/2} = 70$ min [17]) and also for poliovirus-receptor complexes ($k_1 = 1.2 \times 10^7$ $M^{-1}$ $s^{-1}$ and $t_{1/2} = 4.5$ min [2]). These association rate constants are about 10-fold higher than those of protein molecules which form dimers or larger complexes, with $k_1$ values typically in the range of $0.5 \times 10^6$ to $5 \times 10^6$ $M^{-1}$ $s^{-1}$ (26). The high association rates could reflect the highly repetitive arrangement of many receptor binding sites on the virus surface (360 sialic acid binding sites per Py particle [31]) as well as the limited degrees of freedom for the membrane-anchored receptors. In more simple words, when meeting its receptor, the virus does not need to turn around very much to present an attachment site in an orientation complementary to the receptor, which can move and turn in only two dimensions as compared to the three dimensions available for a molecule in solution.

Cell surface sialic acids have been shown to be essential for Py infection (10), and NeuNAc in (α2,3) linkage with galactose (6) has been identified as an essential component of the hemagglutination receptor on erythrocytes. Here we have shown that sialic acids are also necessary for binding to permissive cells. In crystal soaking experiments, Stehle and Harrison (30) determined a dissociation constant of $5 \times 10^{-3}$ to $10 \times 10^{-3}$ M for the binding of sialic acid-(α2,3)-galactose to Py. Low affinities of individual saccharides are a general phenomenon for carbohydrate-protein interactions (34). The dissociation constants of lectins and antibodies with individual saccharides are generally in the millimolar to micromolar range. These low affinities of individual saccharide-protein interactions are in sharp contrast to the high affinities of virus binding to cell surface receptors, which are several orders of magnitude stronger. In the case of Py, we found a $K_d$ value of $1.8 \times 10^{-11}$ M.

However, despite its low affinity, sialic acid has a central role for the Py receptor. This is underlined by the inhibitory effects on Py binding and infection observed here in cells that carry sialic acids with elongated *N*-acyl side chains. The incorporation of approximately 30% modified sialic acids with elongated *N*-acyl group resulted in reduction of binding and infection. For NeuNProp, which, compared to the physiological NeuNAc, carries only a single additional methylene group in the *N*-acyl side chain, we analyzed binding in more quantitative terms and could show that about 28% of high-affinity receptors were absent. This points to a very close interaction between the *N*-acetyl side chain of the neuraminic acid with the virus surface that is efficiently disturbed by the presence of the additional methylene group. Indeed, in the crystal structure of Py virions solved by Stehle et al. (30, 31), the *N*-acetyl side chain of NeuNAc approaches the HI loop and also the BC2 loop of the clockwise neighboring VP1 very closely. Also, our attempts based on the crystal structure to find a position for NeuNProp with binding energies similar to those of NeuNAc failed. Thus, the crystal structure and experimental observation with the modified sialic acids are in good agreement. The structural model could be further validated by generation of VP1 mutants that tolerate NeuNProp in the cellular receptor.

The crucial role of the *N*-acyl side chain for sialylated cellular virus receptors has previously also been observed with two other Pys. Binding and infection of LPV were already negatively affected in NeuNProp-carrying host cells. In contrast, infection by the human polyomavirus BKV was enhanced in NeuNProp-carrying Vero cells, whereas in NeuNPent-carrying cells it was drastically reduced (20). Thus, in three of three sialic acid-dependent virus-receptor interactions analyzed, the *N*-acyl side chain plays a critical role, suggesting that the sialic acid binding structures on the virion surface might be similar in all three viruses. Stehle and Harrison (30) have pointed out that the general topology of the surface of sialic acid binding Py is similar to that of SV40, which apparently does not bind to sialic acid. It remains to be determined whether the sialic acid binding members of the Py family have surface structures in common that are not shared by SV40.

Our finding that the addition of only one methylene group to the *N*-acyl side chain of the sialic acid on an otherwise presumably unmodified receptor structure is sufficient to render the receptor site incapable of infection and high-affinity binding highlights one requirement for receptor structure and specificity that may be easily overlooked; i.e., not only must the virus and receptor have sufficient positive interactions, but also, in the vicinity of the binding surface no steric hindrance is allowed. The large-plaque variant of Py and a branched (α2,3)-(α2,6)-disialyllactose represent an example of this requirement on the viral side. In this strain, the presence of glutamic acid at amino acid 91 of VP1 interferes negatively with the (α2,6)-linked sialic acid, whereas the presence of a glycine residue at this position in the small-plaque strain allows the binding also of this branched oligosaccharide, apparently without additional binding interactions being generated (30).

The $10^8$-fold difference in affinity of Py binding to sialyllactose monomers ($K_d = 5 \times 10^{-3}$ to $10 \times 10^{-3}$ M) versus cell surface receptors ($K_d = 1.8 \times 10^{-11}$ M) clearly shows that in addition to a single sialic acid, other structures must be involved in forming the cell surface receptor. Below we discuss five principal possibilities.

(i) The cell surface oligosaccharide recognized could be monomeric but far more complex than sialyllactose. However, no examples of such high-affinity interactions of a complex oligosaccharide with a protein have been found. As pointed out in a recent review, the affinities resulting from additional oligosaccharide contacts result in $K_d$s in the range of $10^{-6}$ M at best (38).

(ii) Binding occurs to several low-affinity monomeric receptors that move within the plane of the membrane by lateral diffusion and are sequentially recruited in the virus-receptor complex. In view of the high association rate constant at 4°C of $1.7 \times 10^7$ $M^{-1}$ $s^{-1}$ and the very low or absent lateral mobility

of membrane components at this temperature (1), we do not favor this possibility.

(iii) The receptor could be a monomeric sialoglycoprotein, and the majority of the binding energies would be contributed by the interaction of the protein part of the receptor with the virion surface. Indeed, by several different techniques and using mouse kidney cells, Consigli and coworkers have repeatedly identified putative Py receptor proteins with molecular masses of 120 kDa (12) and 95, 50, and 31 to 24 kDa (24, 25). However, so far none of these candidate proteins could be unequivocally identified as the receptor. Our demonstration that sialic acid on 3T6 cells is necessary for binding indicates that the affinity of the putative proteinaceous receptor component alone is not sufficient for binding.

In the next two possibilities, the virion with its multiply repetitive surface recognizes a preformed structure via multiple (three to five?) sialic acid interactions as its receptor.

(iv) The multiple sialic acids could come from a highly branched (antennated) sugar with several terminal sialic acids. However, such sugar structures can be assumed to be rather flexible and therefore should be rather unselective in binding. They probably occur at many cell surfaces and are not easily compatible with the cell type specificity displayed by many sialic acid binding viruses.

(v) The last and, in our view, most appealing possibility is that sialic acids are exposed by the individual members of a homo- or heteropolymeric glycoprotein complex. The polymer backbone itself may not bind to the virus but rather may through its own rigidity function to position terminal sialic acids on short oligosaccharides in the right orientation and spacing on the surface complementary to the highly ordered and fixed arrangement of the viral sialic acid binding sites. To get a rough idea of the spacing postulated by this model, we have calculated the distances between neighboring sialic acid binding sites on the Py surface from the Py structure established by Stehle et al. (31). Within a Py VP1 pentamer, the basic subunit of the viral capsid, neighboring sialic acid binding sites are approximately 32 Å apart, and the distance between sites on neighboring pentamers varies between 52 and 73 Å.

Lee and Lee (22) showed for C-type lectins, which require a calcium ion to exhibit binding activity, that the $K_d$ values decrease from about $10^{-3}$ M for monovalent saccharides to $10^{-5}$ to $10^{-6}$ M for divalent oligosaccharides to $10^{-7}$ to $10^{-8}$ M for synthetic and perhaps suboptimal trivalent structures. Although the mode of binding of the NeuNAc-Py complex differs considerably from the mode of binding for the C-type lectins, it can be speculated that three to six interactions might be sufficient to yield a $K_d$ value of $10^{-11}$ M. The virus surface displays three- and fivefold symmetries which could fit sialic acids exposed by an equally symmetrical backbone. The tight structural requirements for sialic acid positioning could be disturbed in attempts to solubilize sialic acid-dependent viral receptors and thus might help to explain the apparent experimental difficulty in molecularly defining complete sialylated receptor structures.

## ACKNOWLEDGMENTS

We thank H. zur Hausen for continuous support and T. Stehle, J. Langner, M. Goltz, and O. Keppler for helpful discussions. We are very grateful to R. Consigli for the generous gift of Py antibodies and to T. Stehle and S. Harrison for making available the Py structure coordinates.

This work was supported in part by grants from the Bundesministerium für Bildung und Forschung, Bonn, Germany, to W.R. and M.P. and from the Sonnenfeld-Stiftung, Berlin, Germany, to W.R.

## REFERENCES

1. **Anderson, C. M., G. N. Georgiou, I. E. Morrison, G. V. Stevenson, and R. J. Cherry.** 1992. Tracking of cell surface receptors by fluorescence digital imaging microscopy using a charge-coupled device camera. Low-density lipoprotein and influenza virus receptor mobility at 4 degrees C. J. Cell Sci. **101:**415–425.
2. **Bibb, J. A., G. Witherell, G. Bernhardt, and E. Wimmer.** 1994. Interaction of poliovirus with its cell surface binding site. Virology **201:**107–115.
3. **Bolen, J. B., D. G. Anders, J. Trempy, and R. A. Consigli.** 1981. Differences in the subpopulations of the structural proteins of polyoma virions and capsids: biological functions of the multiple VP1 species. J. Virol. **37:**80–91.
4. **Burness, A. T. H.** 1981. Virus receptors (part II), p. 65–84. *In* K. Lonberg-Holm and L. Phillipson (ed.), Receptors and recognition. Chapman and Hall, London, United Kingdom.
5. **Cahan, L. D., and J. C. Paulson.** 1980. Polyoma virus adsorbs to specific sialyloligosaccharide receptors on erythrocytes. Virology **103:**505–509.
6. **Cahan, L. D., R. Singh, and J. C. Paulson.** 1983. Sialyloligosaccharide receptors of binding variants of polyoma virus. Virology **130:**281–289.
7. **Clayson, E. T., and R. W. Compans.** 1988. Entry of simian virus 40 is restricted to apical surfaces of polarized epithelial cells. Mol. Cell. Biol. **8:**3391–3396.
8. **Clayson, E. T., and R. W. Compans.** 1989. Characterization of simian virus 40 receptor moieties on the surfaces of Vero C1008 cells. J. Virol. **63:**1095–1100.
9. **Forstova, J., N. Krauzewicz, S. Wallace, A. J. Street, S. M. Dilworth, S. Beard, and B. E. Griffin.** 1993. Cooperation of structural proteins during late events in the life cycle of polyomavirus. J. Virol. **67:**1405–1413.
10. **Fried, H., L. D. Cahan, and J. C. Paulson.** 1981. Polyoma virus recognizes specific sialyligosaccharide receptors on host cells. Virology **109:**188–192.
11. **Griffin, B. E.** 1981. Structure and genomic organization of SV40 and polyoma virus, p. 61–123. *In* J. Tooze (ed.), DNA tumor viruses. Cold Spring Harbor Laboratory, Cold Spring Harbor, N.Y.
12. **Griffith, G. R., and R. A. Consigli.** 1986. Cross-linking of a polyomavirus attachment protein to its mouse kidney cell receptor. J. Virol. **58:**773–781.
13. **Grünholz, H. J., E. Harms, M. Opetz, W. Reutter, and M. Cerny.** 1981. Inhibition of in vitro biosynthesis of N-acetylneuraminic acid by N-acyl- and N-alkyl-2-amino-2-deoxyhexoses. Carbohydr. Res. **96:**259–270.
14. **Hagler, A. T., E. Huler, and S. Lifson.** 1974. Energy functions for peptides and proteins. Deviation of a consistent force field including the hydrogen bond for amide crystals. J. Am. Chem. Soc. **96:**5316–5327.
15. **Hagler, A. T., S. Lifson, and P. Dauber.** 1979. Consistent force field studies of intermolecular forces in hydrogen-bonded crystals. 2. A benchmark for the objective comparison of alternative force field. J. Am. Chem. Soc. **101:**5122–5130.
16. **Haun, G., O. T. Keppler, C. T. Bock, M. Herrmann, H. Zentgraf, and M. Pawlita.** 1993. The cell surface receptor is a major determinant restricting the host range of the B-lymphotropic papovavirus. J. Virol. **67:**7482–7492.
17. **Herrmann, M., M. Oppenländer, and M. Pawlita.** 1995. Fast and high-affinity binding of B-lymphotropic papovavirus to human B-lymphoma cell lines. J. Virol. **69:**6797–6804.
18. **Kayser, H., C. Ats, J. Lehmann, and W. Reutter.** 1993. New amino sugar analogues are incorporated at different rates into glycoproteins of mouse organs. Experientia **49:**885–887.
19. **Kayser, H., R. Zeitler, C. Kannicht, D. Grunow, R. Nuck, and W. Reutter.** 1992. Biosynthesis of a nonphysiological sialic acid in different rat organs, using N-propanoyl-D-hexosamines as precursors. J. Biol. Chem. **267:**16934–16938.
20. **Keppler, O. T., P. Stehling, M. Herrmann, H. Kayser, D. Grunow, W. Reutter, and M. Pawlita.** 1995. Biosynthetic modulation of sialic acid-dependent virus-receptor interactions of two primate polyoma viruses. J. Biol. Chem. **270:**1308–1314.
21. **Klotz, I. M.** 1982. Numbers of receptor sites from Scatchard graphs: facts and fantasies. Science **217:**1247–1249.
22. **Lee, Y. C., and R. T. Lee.** 1995. Carbohydrate-protein interactions: basis of glycobiology. Acc. Chem. Res. **28:**321–327.
23. **Marriott, S. J., and R. A. Consigli.** 1985. Production and characterization of monoclonal antibodies to polyomavirus major capsid protein VP1. J. Virol. **56:**365–372.
24. **Marriott, S. J., G. R. Griffith, and R. A. Consigli.** 1987. Octyl-beta-D-glucopyranoside extracts polyomavirus receptor moieties from the surfaces of mouse kidney cells. J. Virol. **61:**375–382.
25. **Marriott, S. J., D. J. Roeder, and R. A. Consigli.** 1987. Anti-idiotypic antibodies to a polyomavirus monoclonal antibody recognize cell surface components of mouse kidney cells and prevent polyomavirus infection. J. Virol. **61:**2747–2753.
26. **Northrup, S. H., and H. P. Erickson.** 1992. Kinetics of protein-protein association explained by Brownian dynamics computer simulation. Proc. Natl. Acad. Sci. USA **89:**3338–3342.
27. **Pawlita, M., M. Müller, M. Oppenländer, M. Zentgraf, and M. Herrmann.** 1996. DNA encapsidation by viruslike particles assembled in insect cells from major capsid protein VP1 of B-lymphotropic papovavirus. J. Virol. **70:**7517–7526.

28. **Rickwood, D., and G. D. Birnie.** 1975. Metrizamide: a new density gradient medium. FEBS Lett. **50:**102–110.
29. **Sinibaldi, L., D. Viti, P. Goldoni, G. Cavallo, C. Caroni, and N. Orsi.** 1987. Inhibition of BK virus haemagglutination by gangliosides. J. Gen. Virol. **68:**879–883.
30. **Stehle, T., and S. C. Harrison.** 1996. Crystal structure of murine polyomavirus in complex with straight-chain and branched-chain sialyloligosaccharide receptor fragments. Structure **2:**183–194.
31. **Stehle, T., Y. W. Yan, T. L. Benjamin, and S. C. Harrison.** 1994. Structure of murine polyomavirus complexed with an oligosaccharide receptor fragment. Nature **369:**160–163.
32. **Taylor, N. R., and M. von Itzstein.** 1994. Molecular modeling studies on ligand binding to sialidase from influenza virus and the mechanism of catalysis. J. Med. Chem. **37:**616–624.
33. **Todaro, G. J., and H. Green.** 1963. Development of established mouse lines and their transformation by polyoma virus. Fed. Proc. **22:**382–390.
34. **Toone, E. J.** 1994. Structure and energetics of protein-carbohydrate complexes. Curr. Opin. Struct. Biol. **4:**719–728.
35. **Treisman, R., U. Novak, J. Favaloro, and R. Kamen.** 1981. Transformation of rat cells by an altered polyoma virus genome expressing only the middle-T protein. Nature **292:**595–600.
36. **Watowich, S. J., J. J. Skehel, and D. C. Wiley.** 1994. Crystal structures of influenza virus hemagglutinin in complex with high-affinity receptor analogs. Structure **2:**719–731.
37. **Weis, W., J. H. Brown, S. Cusack, J. C. Paulson, J. J. Skehel, and D. C. Wiley.** 1988. Structure of the influenza virus haemagglutinin complexed with its receptor, sialic acid. Nature **333:**426–431.
38. **Weis, W. I., and K. Drickamer.** 1996. Structural basis of lectin-carbohydrate recognition. Annu. Rev. Biochem. **65:**441–473.
39. **Wieser, J. R., A. Heisner, P. Stehling, F. Oesch, and W. Reutter.** 1996. In vivo modulated N-acyl side chain of N-acetylneuraminic acid modulates the cell contact-dependent inhibition of growth. FEBS Lett. **395:**170–173.